

## **Track-structure simulations of energy deposition patterns to mitochondria and damage to their DNA**

Werner Friedland<sup>1</sup>, Elke Schmitt<sup>1</sup>, Pavel Kundrát<sup>1</sup>, Giorgio Baiocco<sup>2</sup>, Andrea Ottolenghi<sup>2</sup>

*<sup>1</sup>Institute of Radiation Protection, Helmholtz Zentrum München – German Research Center for Environmental Health, Neuherberg, Germany*

*<sup>2</sup>Department of Physics, University of Pavia, Pavia, Italy*

Corresponding author: Werner Friedland, Institute of Radiation Protection, Helmholtz Zentrum München – German Research Center for Environmental Health, Ingolstädter Landstr. 1, 85764 Neuherberg, Germany; +49 89 3187 2767; friedland@helmholtz-muenchen.de

# Track-structure simulations of energy deposition patterns to mitochondria and damage to their DNA

## Abstract

**Purpose:** Mitochondria have been implicated in initiating and/or amplifying the biological effects of ionizing radiation not mediated via damage to nuclear DNA. To help elucidate the underlying mechanisms, energy deposition patterns to mitochondria and radiation damage to their DNA have been modelled.

**Methods:** Track-structure simulations have been performed with PARTRAC biophysical tool for  $^{60}\text{Co}$  gamma-rays and 5 MeV alpha-particles. Energy deposition to the cell's mitochondria has been analyzed. A model of mitochondrial DNA reflecting experimental information on its structure has been developed and used to assess its radiation-induced damage.

**Results:** Energy deposition to mitochondria is highly inhomogeneous, especially at low doses. Although a dose-dependent fraction of mitochondria sees no energy deposit at all, the hit ones receive rather high amounts of energy. Nevertheless, only little damage to mitochondrial DNA occurs, even at large doses.

**Conclusion:** Mitochondrial DNA does not represent a critical target for radiation effects. Likely, the key role of mitochondria in radiation-induced biological effects arises from the communication between mitochondria and/or with the nucleus. Through this signaling, initial modifications in a few heavily hit mitochondria seem to be amplified to a massive long-term effect manifested in the whole cell or even tissue.

194/200 words

**Keywords:** Track-structure simulations, microdosimetry, mitochondria, DNA damage, DOREMI

**Running title:**

Simulation of radiation damage to mitochondria

## Introduction

The vast majority of human cells' energy is produced in mitochondria, double-membrane organelles of spherical or ellipsoidal shape and sizes of 0.5 – 1  $\mu\text{m}$ . In agreement with the diverse energy needs, the numbers of mitochondria vary widely among cell types; human erythrocytes do not contain any, whereas muscle (including heart) or liver cells may contain thousands of these organelles. Mitochondria are highly mobile in terms of their shape as well as position but may also stay fixed at intracellular locations where energy is needed, e.g. close to the contractile apparatus in cardiac muscle cells (Alberts et al. 2013, Alberts et al. 2014). Mitochondria also serve as calcium buffers and metabolic signaling centers in general; they are also involved in intercellular communication. A central part of the energy conversion system in mitochondria is the electron transport chain; through its leakage, mitochondria are sources of reactive oxygen species (ROS) that play a role in signaling processes but may also damage lipids, proteins, and DNA. Mitochondrial functions are tightly regulated, both within a cell and beyond its boundaries. Mitochondrial dysfunctions have been identified in aging as well as in a large variety of diseases including metabolic disorders, diabetes, cancer or neurodegenerative disorders such as Parkinson's or Alzheimer's diseases (Wallace 2005, Nunnari and Suomalainen 2012). Mitochondria possess their own DNA (mtDNA), in humans inherited maternally, as well as a complete transcriptional and translational system including ribosomes that enables them to produce their own proteins (Alberts et al. 2013); mtDNA encodes 37 genes for the key proteins of the electron transport chain, the others being encoded in nuclear DNA. Mutations in mtDNA are linked to a variety of diseases (Schon et al. 2012).

Mitochondria have also been widely implicated in short- and long-term biological effects of ionizing radiation, *in vitro* and *in vivo* (Leach et al. 2001, Kim et al. 2006, Nugent et al. 2010, Rajendran et al. 2011, Yamamori et al. 2012, Kam and Banati 2013). Converging

lines of evidence suggest that mitochondria, their network, and interactions with the nucleus play a pivotal role in the induction and persistence of oxidative stress post irradiation as well as in the resulting epigenetic changes and genomic instability, identified among critical traits of cancer (Szumiel 2015). Mitochondria may initiate and/or amplify bystander signaling (Chen et al. 2008, Chen et al. 2009, Hanot et al. 2009, Prise and O'Sullivan 2009, Rajendran et al. 2011). Mitochondrial proteins represent the protein class showing the strongest response to irradiation in mice heart tissue at 24 hours and after weeks or months (Azimzadeh et al. 2011, Barjaktarovic et al. 2011, Azimzadeh et al. 2013, Barjaktarovic et al. 2013); modified gene and protein expressions have been seen already at doses as low as 0.2 Gy. Radiation effects to mitochondria in human cardiac muscle cells may be of particular interest in breast cancer radiation therapy, which inevitably leads to considerable dose burden to the heart.

Open questions not elucidated sufficiently so far are to what extent mitochondria alone or specifically their DNA represent critical initial targets of those radiation effects that are not mediated by hits to nuclear DNA, and what the role of the communication among mitochondria and/or with the nucleus is. To address these issues from first principles, energy deposition patterns in mitochondria and radiation-induced damage to mtDNA have been estimated by simulations with the PARTRAC tools (Friedland et al. 2011a). Earlier investigations, aimed at a mechanistic interpretation of bystander effects in medium transfer experiments, demonstrated that specific energy, the microscopic analogue of absorbed dose (ICRU 1983), deposited to heavily hit mitochondria may exceed the applied mean dose by several orders of magnitude (Friedland et al. 2011b, Kundrat and Friedland 2012). In this work, conceptually similar simulations have been performed for  $^{60}\text{Co}$   $\gamma$ -rays as an exemplary photon and for 5 MeV  $\alpha$ -particles as an exemplary ion irradiation, for doses ranging from 2 mGy to 2 Gy. Regarding radiation damage to mtDNA, a detailed model of mtDNA structure has been developed, representing the experimental information and making use of

the tools previously employed for modelling nuclear DNA and chromatin structures. Yields of radiation-induced damage to mtDNA and the resulting fragmentation patterns are reported, explicitly accounting for direct and indirect (radical-mediated) effects, for  $^{60}\text{Co}$   $\gamma$ -rays and for 5 MeV  $\alpha$ -particles. The results suggest that mtDNA does not represent a critical target for radiation effects, and support the hypothesis that initial effects (presumably, oxidative stress) in a few heavily hit mitochondria are amplified through inter-mitochondrial and/or mitochondria-nucleus signaling to long-term effects on cellular and/or tissue-level scales.

## **Methods**

### ***Modelling energy deposition patterns in mitochondria***

Simulations of energy deposition patterns have been performed using the biophysical modelling tool PARTRAC. The principal application area of PARTRAC includes simulating track structures of diverse radiation types, DNA damage induction in cell nuclei, its repair, and the formation of chromosome aberrations (Friedland et al. 2011a, Friedland and Kundrat 2013, Schmid et al. 2015, Friedland et al. 2017). However, PARTRAC can be used for micro- and nanodosimetric calculations too. Previously, energy deposition patterns have been calculated in subcellular targets such as mitochondria or membranes (Friedland et al. 2011b, Kundrat and Friedland 2012), aimed at a mechanistic explanation of the observed threshold dose of 2-3 mGy for bystander effects in medium transfer experiments (Liu et al. 2007). It was found that in an ensemble of many thousand cells, some sub-cellular volumes of mitochondrial size will receive specific energies ('local doses') of several Gy, although the applied (macroscopic) dose is lower by 3 orders of magnitude.

In the present study, distributions of specific energies to mitochondria and cell nuclei have been determined for  $^{60}\text{Co}$   $\gamma$ -ray and 5 MeV  $\alpha$ -particle irradiation. Distributions of specific energies due to  $\gamma$ -rays were analyzed for low (2 mGy, 20 mGy) and

intermediate/higher (0.2 Gy, 2 Gy) doses. For  $\alpha$ -particles, at low doses the specific energy per hit mitochondrion does not change but only the fraction of hit mitochondria increases with the dose; hence, the results have been analyzed for single  $\alpha$ -particles and for 1 Gy dose. For both  $\gamma$ - and  $\alpha$ -particle irradiations, tracks of the primary particles and their secondary electrons have been simulated event-by-event in liquid water, which has been used as a surrogate for biologically relevant medium. To limit computational expenses for  $\gamma$ -irradiation, photon and electron tracks were traced inside a 'world' cube with 58.6  $\mu\text{m}$  edge length and reflected at the surface layers so that for each  $^{60}\text{Co}$   $\gamma$  its mean energy of 1.255 MeV has been completely deposited inside this world cube, corresponding to a dose increment of 1 mGy under electronic equilibrium conditions. The total number of photons simulated per run has been determined by the dose studied (2 mGy – 2 Gy); totally 100.000 photons with all their secondary electrons have been studied. For the analysis of energy deposit in nuclei and mitochondria, ionizations and excitations have been recorded inside a cubic target volume of 12.5  $\mu\text{m}$  side length, concentric to the world cube. This target cube has been virtually filled with 8 spheres representing nuclei of 125  $\mu\text{m}^3$  volume or 1728 spheres representing mitochondria of 0.5  $\mu\text{m}^3$  volume; i.e. locations of ionizations and excitations have been associated to a nucleus or a mitochondrion whenever the distance to its center has been below the radius of 3.1  $\mu\text{m}$  or 0.49  $\mu\text{m}$ , respectively. The energy deposits in individual nuclei or mitochondria have been estimated from the average energy deposit per ionization and excitation event, 14.92 eV, including 2.75 eV from subexcitation electrons; finally, the energy deposits have been converted to specific energies (1 Gy in water corresponds to 6.24 keV/ $\mu\text{m}^3$ ). For  $\alpha$ -particles, the same setup has been used, but the tracks have not been mirrored at the surface layers; i.e. single track segments with a linear energy transfer (LET) of about 95 keV/ $\mu\text{m}$  have been modelled and analyzed separately, or as corresponding to a mean dose of 1 Gy resulting from a fluence of 0.061 particles per  $\mu\text{m}^2$ .

### ***Modelling radiation-induced damage to mtDNA***

DNA damage to nuclear DNA and chromatin is scored in biophysical simulations by overlapping the track structures of photons, electrons, protons or heavier ions with sophisticated multi-scale models of the target structures. Direct damage results from energy deposition events in the volume of DNA. Events outside DNA are processed via pre-chemical and chemical modules of the code, which simulate the formation of radicals from water radiolysis, as well as their diffusion and mutual reactions. Attacks of the radicals onto DNA are scored as indirect DNA damage. Details on model assumptions and parameters such as energy needed to induce a strand break in DNA double-helix or the incorporated radical reactions can be found in (Friedland et al. 2011a, Friedland and Kunderát 2014).

To extend this approach to mtDNA, an mtDNA model for DNA damage simulations with PARTRAC has been developed, reflecting its known structure (Hallberg and Larsson 2011, Kukat et al. 2011, Bogenhagen 2012, Alexeyev et al. 2013, Kukat and Larsson 2013, Kukat et al. 2015): An mtDNA molecule consists of a closed loop of 16,569 bp (base pair) DNA double-helix. It is almost fully coated by mitochondrial transcription factor A (TFAM) proteins which impose frequent 180° U-turns on mtDNA; there are about 1000 TFAM molecules per mtDNA, i.e. on average one TFAM molecule per 16.6 bp (Kukat et al. 2011). The packaging of mtDNA is not an ordered, repetitive process as in nuclear DNA bound to nucleosomes and forming the 30 nm chromatin fiber but follows an almost random pattern, with a high degree of TFAM clustering (Kukat et al. 2015). These frequent U-turns and the cross-strand binding of TFAM compact the mtDNA into mitochondrial nucleoids; nucleoids most frequently contain only single mtDNA molecules (Kukat et al. 2011, Kukat et al. 2015). Super-resolution microscopy images have shown that these nucleoids possess ellipsoidal, almost spherical shapes with apparent sizes of about 100 nm, corresponding to actual sizes (after deducing the size of bound antibodies) of about 70 nm (Kukat et al. 2011, Kukat et al.

2015). A mitochondrion typically contains several nucleoids; up to a few thousands mitochondria may be found in energetically highly active cells such as heart muscle cells.

Following this experimental information, the PARTRAC model of mtDNA and mitochondria has been developed as follows: Five distinct cubic boxes of 15 nm edge length have been generated, containing 318-326 bp DNA with U-turns every about 15-20 bp. A straight box in which the mtDNA connects the bottom and top walls is illustrated in Figure 1A; in the other boxes, mtDNA bends to the left, right, front or back, respectively. These boxes have been constructed by adapting the standard PARTRAC chromatin boxes of 50 nm size as used in chromatin modelling (Friedland et al. 2011a), replacing histone molecules by TFAM proteins and adjusting the winding angles, protein numbers, and sizes appropriately. By seamlessly stacking 52 such boxes into a compact loop with ~60 nm size (Figure 1B) of a slightly prolonged shape, a closed mtDNA loop of 16.7 kbp length has been built. Ten such mtDNA copies (10 nucleoids) have been placed in close vicinity within a sphere with 1  $\mu\text{m}$  diameter that has served as a model mitochondrion; no internal structures such as double membrane or cristae have been considered. Finally, 1000 mitochondria have been positioned randomly in the cytoplasm of a model heart cell (sphere with diameter of 20  $\mu\text{m}$ , concentric spherical nucleus of 10  $\mu\text{m}$  diameter, Figure 1C). The model cell thus contains in total 167 Mbp mtDNA (which corresponds about to the mean size of a human chromosome) and 6.6 Gbp nuclear DNA. Due to the high number of mitochondria per cell and mtDNA molecules per mitochondrion included, the given model may be viewed as a semi-realistic model of energetically highly active cells such as heart muscle or liver cells, serving at the same time as an upper limit on mtDNA-related effects in less active cells.

To assess radiation-induced mtDNA damage, the given model cell with 1000 mitochondria per cell and 10 mtDNA molecules per mitochondrion has been overlaid with tracks of  $^{60}\text{Co}$   $\gamma$ -rays. To further study the radiation quality-dependence of the assessed

effects, 5 MeV  $\alpha$ -particles have also been simulated. Direct DNA damage from energy depositions within mtDNA have been scored as standardly done in PARTRAC for nuclear DNA (Friedland et al. 2011a). Regarding indirect effects mediated by reactive species, alternative scenarios have been considered to account for the unknown degree of radical scavenging in mitochondria: The mtDNA, originally considered to be naked and vulnerable to damage, has been later shown to be coated by proteins and aggregated into nucleoids (Kukat et al. 2011). Nuclear DNA is known to be protected by histones and also by general scavengers such as glutathione; in PARTRAC, histones are represented explicitly in atomic resolution, and lifetimes of hydroxyl radicals of 2.5 ns are taken in the nucleus, based on corresponding experimental data, see (Friedland et al. 2011a) and references therein. To the knowledge of the authors, no such detailed information is available for mitochondria and mtDNA. Therefore, for indirect damage to mtDNA, specific scavenging by TFAM and/or other proteins coating mtDNA has not been considered explicitly, but included in the effective lifetime of hydroxyl radicals in mitochondria, for which three alternative scenarios have been evaluated: Lifetime of 2.5 ns as in nuclear environment; no additional scavenging of  $\cdot\text{OH}$  but only reactions with DNA constituents and products of water radiolysis; and complete scavenging with lifetime of 0 ns, i.e. direct effects only with no damage through radical attacks. Induction of single- and double-strand breaks (SSB, DSB) or more complex lesions and fragmentation patterns in mtDNA have been scored using methods previously developed for nuclear DNA (Friedland et al 2011a), modified to account for the closed-loop structure of mtDNA. For both radiation types studied, 1000 simulations have been done with mtDNA (and 20 simulations with nuclear DNA) until in each run energy deposits in the model cell corresponding to the dose of 10 Gy have been obtained. While the damage yields are reported per unit dose, the fragmentation patterns refer to a single track.

## Results

### *Energy deposition to mitochondria*

The stochastic and quantum nature of ionizing radiation, and in particular the specific spatial structure of ion tracks, leads to inhomogeneous specific energy ('local dose') distributions on cellular or subcellular scales. This inhomogeneity increases with decreasing target size and/or decreasing dose. Since mitochondria are considerably smaller than cell nuclei, the inhomogeneity may be an issue for these organelles but of no concern for cell nuclei at low or moderate mean doses.

To address this issue in detail, the distribution of specific energies in an ensemble of nuclei and mitochondria has been investigated for  $^{60}\text{Co}$   $\gamma$ - and 5 MeV  $\alpha$ -particle irradiation at doses from 2 mGy to 2 Gy. In Figure 2, the cumulative distribution of specific energy deposited by  $^{60}\text{Co}$   $\gamma$ -irradiation to mitochondria with  $0.5 \mu\text{m}^3$  volume is shown in comparison with the corresponding distribution for cell nuclei of  $125 \mu\text{m}^3$  volume (note that this value is close to the volume, about  $150 \mu\text{m}^3$ , actually filled with DNA fiber boxes in the multi-scale model of cell nucleus used in PARTRAC simulations of nuclear DNA damage, although the whole nucleus comprises a larger sphere of  $524 \mu\text{m}^3$  volume). Panel A shows the cumulative distribution of specific energies to mitochondria (solid lines) or cell nuclei (dotted lines); plotted are the fractions of targets receiving specific energy below the abscissa values. A single energy deposit (as discussed above, mean energy deposit of 14.92 eV) per  $0.5 \mu\text{m}^3$  mitochondrion means specific energy of about 4.8 mGy; in the semi-logarithmic plot in Figure 2A, non-hit mitochondria (which by definition see specific energy of 0 mGy) have been depicted by the leftmost histogram segment (segment below 4.8 mGy). At 2 Gy dose, virtually all mitochondria are hit; they receive specific energies ranging from  $\sim 0.4$  up to  $\sim 6$  Gy. At 0.2 Gy dose, 7% of the mitochondria are not hit. This non-hit fraction increases to 75% and 97% at 20 mGy and 2 mGy, respectively. The corresponding distributions for cell

nuclei (dotted lines) show considerably lower inhomogeneity; again, the inhomogeneity increases with decreasing dose. For 2 mGy mean dose, about 22% of the nuclei receive no energy deposit (not shown); a single energy deposition event within the cell nucleus corresponds to ~0.02 mGy specific energy on average. In panel B, the same results are plotted in log-log scale; whereas the accumulation towards larger doses in panel A points out the width of the target dose distribution and the fraction of targets without hits, the accumulation towards lower doses in panel B emphasizes the fraction of targets receiving relatively high specific energies ('local doses') in spite of low ('macroscopic') doses: For instance, one mitochondrion out of 1000 receives specific energy of at least 0.4 Gy, 1.5 Gy, 2.8 Gy and 6.8 Gy at applied doses of 2 mGy, 20 mGy, 0.2 Gy and 2 Gy, respectively. Thus, the specific energies seen within a small group of highly exposed organelles change by about a factor of two to four only although the dose varies by a factor of ten.

For 5 MeV  $\alpha$ -particles, it is mainly the fraction of hit nuclei and/or mitochondria that is changing with varying dose, but not the specific energy seen by the targets. Hence, the corresponding results for  $\alpha$ -particles are presented in Figure 3 for a mean dose of 1 Gy and for a single particle traversal; in this latter case only targets that received at least one energy deposit have been included in the analysis. At 1 Gy, about 94% of the mitochondria and about 10% of the cell nuclei are not hit (Figure 3A). For the mitochondria that have been hit, the distribution of specific energy is rather similar to the single particle distribution (Figure 3B), except at specific energies above 40 Gy which occur in about 1 out of 1000 targets due to two (or more) tracks hitting the same target. The specific energy to the nucleus deposited by a single track ranges from 0.1 to almost 1 Gy (Figure 3A). Thus, at 1 Gy dose, the nucleus is usually hit by multiple tracks; the specific energy to the nucleus does not exceed 4 Gy in this case.

The distributions shown are exemplary results for photon and for ion irradiation. Test simulations have shown that for lower photon energies the inhomogeneity becomes larger; however, a detailed analysis is outside the scope of the present work. For ion irradiation, the linear energy transfer (LET) is a major descriptor of radiation quality and also of the inhomogeneity in specific energy. Essential characteristics of the specific energy distribution can be roughly estimated under the simplifying assumption that all interactions due to the ion with LET  $L$  are located on a straight line. Then, the mean dose  $D$  due to a single traversal through a spherical volume with cross-sectional area  $A$  is given by

$$D [\text{Gy}] = 0.1602 L [\text{keV}/\mu\text{m}]/A [\mu\text{m}^2];$$

the numerical factor follows from unit conversion. For an  $\alpha$ -particle of 5 MeV energy the LET is about 95 keV/ $\mu\text{m}$ ; this leads to a mean specific energy of 0.5 Gy per nuclear traversal and 20 Gy per mitochondrial traversal. As the maximum chord length exceeds its mean value by a factor of 1.5 (since the mean chord length of a sphere is  $2/3$  of its diameter), the corresponding maximal values of specific energy are about 0.75 Gy and 30 Gy for nuclear and mitochondrial traversals. The fraction  $f(n)$  of targets that encounters a number  $n$  of traversals through its volume, given that the mean number of traversals is  $a$ , follows a Poisson distribution:

$$f(n) = a^n \exp(-a) / n!$$

For the mean dose values per traversal given above the parameter  $a$  equals 1 and the fraction of no traversal is 36.8%. Since  $a$  scales linearly with dose, the fraction of non-hit targets  $f(0)$  can be easily deduced for further dose values: according to the estimation above about 13.5% of the nuclei ( $a = 2$ ) and 95% of the mitochondria ( $a = 0.05$ ) are not hit by the  $\alpha$ -track at 1 Gy dose. These values, as well as the mean specific energies per particle traversal, are in overall

agreement with the results of the detailed analysis.

### ***Damage to mtDNA***

The yields of single- and double-strand breaks (SSB, DSB) in mtDNA upon  $^{60}\text{Co}$   $\gamma$ - or 5 MeV  $\alpha$ -irradiation simulated by PARTRAC are reported in Table 1. Three cases are considered here, namely with hydroxyl radical ( $\cdot\text{OH}$ ) lifetime of 2.5 ns as in the nucleus (Friedland et al. 2011a), without scavenging of  $\cdot\text{OH}$  in mitochondria despite interactions with mtDNA, and without indirect effects due to  $\cdot\text{OH}$  attack. For comparison, also the data on DNA damage in nuclear DNA (nDNA) are listed. DNA damage from energy deposition events within the molecule is scored as direct damage, contrary to indirect one which is mediated by  $\cdot\text{OH}$  attacks (whereby indirect DSB include those DSB where at least one of the strand breaks is induced by  $\cdot\text{OH}$ ). The yields of direct damage in mtDNA and nDNA are almost identical. This result could have been anticipated since the basic molecular structure (i.e. the double-helix) is the same and differences due to dissimilar bending of the helix have only marginal impact on the effective target volume per base pair.

The indirectly induced damage increases if the degree of scavenging decreases (i.e.  $\cdot\text{OH}$  lifetime increases). The simulated indirect (and hence also the total) damage is larger in mtDNA than in nDNA for both nucleus-like and low scavenging in mitochondria. The reason is that mtDNA lacks the protecting histones, and the TFAM proteins have not been assigned a protective role in our model. Due to this simplifying assumption, the results provide an upper limit on the possible mtDNA damage; the realistic figures may be significantly smaller due to the protective role of mtDNA-coating proteins. Nevertheless, even the reported, limiting total damage yields are rather small. Even under low scavenging conditions, much less than 1 % mtDNA will experience a DSB at 1 Gy of  $^{60}\text{Co}$   $\gamma$ - or 5 MeV  $\alpha$ -irradiation (e.g. for  $\alpha$ -

irradiation assuming low scavenging in mitochondria,  $26 \text{ DSB Gy}^{-1} \text{ Gbp}^{-1} \times 1 \text{ Gy} \times 16.7 \text{ kbp}$  per mtDNA = 0.042 % DSB induction probability per mtDNA at 1 Gy dose).

For  $^{60}\text{Co}$   $\gamma$ -irradiation, the DSB are induced fully at random (results not shown), as is typical for low-LET radiation. For 5 MeV  $\alpha$ -particles (LET  $\sim 95 \text{ keV}/\mu\text{m}$ ), however, often more than a single DSB occurs at a single mtDNA molecule, so that two (or even more) fragments are formed from the circular mtDNA. In Figure 4, calculated fragmentation patterns are shown for 5 MeV  $\alpha$ -irradiated mtDNA and nDNA. Characteristic peaks at around 75 bp are seen for nDNA, corresponding to the  $\alpha$ -particle track crossing both helices wound around the histone within a nucleosome. No such clear peaks are predicted for the present mtDNA model, in agreement with the hypothesis that no regular, repetitive structures such as nucleosomes and 30 nm chromatin fiber are formed by the mtDNA. Yet are fragments shorter than about 120 bp relatively frequent in mtDNA, which corresponds to the frequent U-turns around the TFAM proteins and the overall highly compact structure of mtDNA, which is often traversed by the  $\alpha$ -particle track twice within this short genomic interval.

## **Discussion and conclusion**

The PARTRAC simulations on damage to mtDNA have revealed rather small radiation effects. A novel model representing the structure of mitochondrial DNA has been developed. Following experimental information, the model contains a closed 16.7 kbp DNA double-helix in atomic resolution, which shows frequent turns imposed by bound TFAM proteins and forms a compact 60 nm nucleoid. Each mitochondrion contains several nucleoids (10 in the reported simulations). Energetically active cells such as cardiac muscle or liver cells include a high number of mitochondria per cell (1000 in this study). This model has been used to assess radiation-induced damage to mtDNA. Effects mediated by direct energy deposition are

almost identical in mitochondrial and nuclear DNA, since atomic-scale structure of the DNA helices are very similar. Regarding indirect effects mediated by radical attacks, three exemplary degrees of scavenging have been evaluated, since solid information is absent on  $\cdot\text{OH}$  lifetime in mtDNA nucleoids and the degree of mtDNA protection by TFAM and/or other proteins coating this molecule. The PARTRAC predictions on total damage yields in mtDNA upon  $\gamma$ -irradiation,  $185 \text{ SSB Gy}^{-1} \text{ Gbp}^{-1}$  under nucleus-like scavenging conditions (Table 1), compare favorably with the scarce experimental data available,  $(134 \pm 20) \text{ SSB Gy}^{-1} \text{ Gbp}^{-1}$  (May and Bohr 2000). Actually, this comparison suggests slightly smaller  $\cdot\text{OH}$  effects (i.e. stronger scavenging) in mitochondria than in nucleus, consistent with the high coverage of mtDNA by TFAM (Kukat et al. 2015); nevertheless, the reported 2:1 ratio between mitochondrial and nuclear DNA damage (May and Bohr 2000) would imply lower scavenging in mitochondria than in nucleus. Further dedicated research would be needed to elucidate this issue and define a relevant scenario. Nevertheless, in general the simulations complement the experimental data and provide useful estimates on the yields of damage to mtDNA in dependence on applied dose or radiation quality. The simulations show that 5 MeV  $\alpha$ -particles are more effective and also less sensitive to the degree of scavenging than  $^{60}\text{Co}$   $\gamma$ -irradiation. For both radiation types, the vast majority of mtDNA molecules are not affected at all by low or medium doses; at 1 Gy, there is a 1:3000 – 1:6000 chance for a given mtDNA copy to experience a DSB. These small radiation effects are further reduced by DNA repair, which is present even in mtDNA, though less efficient than in nuclear DNA (May and Bohr 2000). On the other hand, when a particular mtDNA molecule is hit, then there are typically multiple DSB, fragmenting the molecule. The predicted mtDNA fragmentation patterns reflect its compact packaging with frequent, random U-turns, contrary to nucleosome-related peaks of 70 – 80 bp in nuclear DNA (Figure 4). However, taken together, the performed mechanistic simulations do not provide support for the hypothesis that mtDNA

were a key target for initial radiation effects.

On the contrary, it is well established that mitochondria do play an important role in initiating and/or amplifying radiation effects, both *in vitro* and *in vivo* (Leach et al. 2001, Kim et al. 2006, Chen et al. 2008, Chen et al. 2009, Hanot et al. 2009, Prise and O'Sullivan 2009, Nugent et al. 2010, Azimzadeh et al. 2011, Barjaktarovic et al. 2011, Rajendran et al. 2011, Yamamori et al. 2012, Azimzadeh et al. 2013, Barjaktarovic et al. 2013, Kam and Banati 2013, Szumiel 2015). In their *in vitro* experiments, Leach et al. (2001) demonstrated a transient increase of ROS production by mitochondria observable at 1 – 5 min post irradiation, with a binary, yes/no response of the whole cell; the percentage of non-responding cells decreased exponentially with dose in agreement with the target theory. The mechanism suggested by the authors was that ionizing radiation induced an oxidative effect in a mitochondrion that led to the release of  $\text{Ca}^{2+}$  which was taken up by neighboring mitochondria and induced their permeability transition, depolarization, ROS production and further  $\text{Ca}^{2+}$  release, leading to signal propagation and amplification. Brady et al. (2004) and Zorov et al. (2006) demonstrated such processes directly; they observed a wave of depolarization in a cell's mitochondria population that was propagating with the speed of 5  $\mu\text{m}/\text{min}$  or cell-wide fluctuations in mitochondria membrane potential with a period of 3 – 10 min. These results show that mitochondria do not act in an isolated manner but are mutually closely interlinked; likewise, communication exists between mitochondria and the nucleus, in both directions.

Exposure to ionizing radiation leads to practically immediate (within  $\mu\text{s}$  time scales) induction of ROS by radiolysis. This ROS induction is rather limited compared to their physiological production rates; e.g. upon 10 mGy irradiation these immediately formed ROS may correspond to their physiological production over around 0.2 s only, averaged over a cell (Mikkelsen and Wardman 2003). However, as shown in this work, energy deposition on sub-

$\mu\text{m}$  scales is highly inhomogeneous, and while most mitochondria in a cell would not receive any energy from such a low-dose irradiation, the few hit ones would see considerably high specific energies ('local doses'). For these simulations, the detailed mtDNA model discussed above was not necessary; it was sufficient to score energy deposits in small spheres, ellipsoids or cylinders, as generally done in approaches proposed so far to address the role of mitochondria in initiating or mediating the biological effects of ionizing radiation (Friedland et al. 2011b, Kundrat and Friedland 2012, Kam and Banati 2013, Kirkby and Ghasroddashti 2015). The results have shown that for instance for  $0.5\mu\text{m}^3$  mitochondria (diameter  $\sim 1\ \mu\text{m}$ ) at 20 mGy of  $^{60}\text{Co}$   $\gamma$ , 1 out of 1000 mitochondria would receive specific energy i.e. 'see a local dose' of  $\sim 1.5$  Gy, which is 75-fold higher than the applied dose. In the case of 5 MeV  $\alpha$ -particles, at doses up to a few Gy most mitochondria see no energy deposit but a hit mitochondrion receives about 20 Gy specific energy (about 60 keV deposited energy), producing about 600  $\text{H}_2\text{O}_2$  molecules. We speculate that these ROS formed immediately upon irradiation in such heavily hit mitochondria may be sufficient to shift the organelle to a state with high ROS release; bistability of the mitochondrial respiratory chain i.e. its ability to operate in two stable states, one with a low and another with a high production of ROS, has been reported (Selivanov et al. 2011). The enhanced production of ROS may lead to opening the mitochondria permeability transition pore, release of cytochrome c, ROS and/or  $\text{Ca}^{2+}$  into the cytoplasm, which may trigger an avalanche reaction in neighbor mitochondria. For details on these and alternative amplification processes, we refer to Mikkelsen and Wardman (2003) and references therein.

Taken together, the reported modelling studies on damage to mitochondrial DNA have shown only little radiation-induced effects, indicating that mitochondrial DNA is not likely a critical target of ionizing radiation. The simulations on energy deposition patterns indicate a large inhomogeneity in specific energy ('local dose') deposited to mitochondria,

especially at low doses or for high-LET radiation. At low doses, most mitochondria are not hit at all, but a few heavily hit ones receive specific energies that are orders of magnitude higher than the applied dose. Presumably, initial effects in such heavily hit mitochondria are then amplified through signaling between mitochondria and/or with the nucleus, so that long-term effects on cellular or even tissue levels arise.

### ***Funding:***

The research leading to these results has received funding from the European Atomic Energy Community's Seventh Framework Programme (FP7/2007–2011) under grant agreement n° 249689 (DoReMi).

### ***Disclosure of interest:***

The authors report no conflicts of interest.

### ***References***

- Alberts, B., D. Bray, K. Hopkin, A. Johnson, J. Lewis, M. Raff, K. Roberts and P. Walter (2013). Essential Cell Biology, Fourth Edition, Taylor & Francis Group.
- Alberts, B., A. Johnson, J. Lewis, D. Morgan, M. Raff, K. Roberts and P. Walter (2014). Molecular Biology of the Cell, Sixth Edition, Taylor & Francis Group.
- Alexeyev, M., I. Shokolenko, G. Wilson and S. LeDoux (2013). "The maintenance of mitochondrial DNA integrity--critical analysis and update." Cold Spring Harb Perspect Biol **5**(5): a012641.
- Azimzadeh, O., H. Scherthan, H. Sarioglu, Z. Barjaktarovic, M. Conrad, A. Vogt, J. Calzada-Wack, F. Neff, M. Aubele, C. Buske, M. J. Atkinson and S. Tapio (2011). "Rapid proteomic remodeling of cardiac tissue caused by total body ionizing radiation." Proteomics **11**(16): 3299-3311.
- Azimzadeh, O., W. Sievert, H. Sarioglu, R. Yentrapalli, Z. Barjaktarovic, A. Sriharshan, M. Ueffing, D. Janik, M. Aichler, M. J. Atkinson, G. Multhoff and S. Tapio (2013). "PPAR alpha: a novel radiation target in locally exposed Mus musculus heart revealed by quantitative proteomics." J Proteome Res **12**(6): 2700-2714.
- Barjaktarovic, Z., D. Schmaltz, A. Shyla, O. Azimzadeh, S. Schulz, J. Haagen, W. Dorr, H. Sarioglu, A. Schafer, M. J. Atkinson, H. Zischka and S. Tapio (2011). "Radiation-induced signaling results in mitochondrial impairment in mouse heart at 4 weeks after exposure to X-rays." PLoS One **6**(12): e27811.
- Barjaktarovic, Z., A. Shyla, O. Azimzadeh, S. Schulz, J. Haagen, W. Dorr, H. Sarioglu, M. J. Atkinson, H. Zischka and S. Tapio (2013). "Ionising radiation induces persistent alterations in the cardiac mitochondrial function of C57BL/6 mice 40 weeks after local heart exposure." Radiother Oncol **106**(3): 404-410.
- Bogenhagen, D. F. (2012). "Mitochondrial DNA nucleoid structure." Biochim Biophys Acta **1819**(9-10): 914-920.
- Brady, N. R., S. P. Elmore, J. J. van Beek, K. Krab, P. J. Courtoy, L. Hue and H. V. Westerhoff (2004). "Coordinated behavior of mitochondria in both space and time: a reactive oxygen species-activated wave of mitochondrial depolarization." Biophys J **87**(3): 2022-2034.

Chen, S., Y. Zhao, W. Han, G. Zhao, L. Zhu, J. Wang, L. Bao, E. Jiang, A. Xu, T. K. Hei, Z. Yu and L. Wu (2008). "Mitochondria-dependent signalling pathway are involved in the early process of radiation-induced bystander effects." *Br J Cancer* **98**(11): 1839-1844.

Chen, S., Y. Zhao, G. Zhao, W. Han, L. Bao, K. N. Yu and L. Wu (2009). "Up-regulation of ROS by mitochondria-dependent bystander signaling contributes to genotoxicity of bystander effects." *Mutat Res* **666**(1-2): 68-73.

Friedland, W., M. Dingfelder, P. Kundrať and P. Jacob (2011a). "Track structures, DNA targets and radiation effects in the biophysical Monte Carlo simulation code PARTRAC." *Mutat Res* **711**(1-2): 28-40.

Friedland, W., P. Kundrať and P. Jacob (2011b). "Track structure calculations on hypothetical subcellular targets for the release of cell-killing signals in bystander experiments with medium transfer." *Radiat Prot Dosimetry* **143**(2-4): 325-329.

Friedland, W. and P. Kundrať (2013). "Track structure based modelling of chromosome aberrations after photon and alpha-particle irradiation." *Mutat Res* **756**(1-2): 213-223.

Friedland, W. and P. Kundrať (2014). Modeling of radiation effects in cells and tissues. *Comprehensive Biomedical Physics*. A. Brahme. Amsterdam, Elsevier. **Vol. 9**: 105-142.

Friedland, W., E. Schmitt, P. Kundrať, M. Dingfelder, G. Baiocco, S. Barbieri and A. Ottolenghi (2017). "Comprehensive track-structure based evaluation of DNA damage by light ions from radiotherapy-relevant energies down to stopping." *Sci Rep* **7**: 45161.

Hallberg, B. M. and N. G. Larsson (2011). "TFAM forces mtDNA to make a U-turn." *Nat Struct Mol Biol* **18**(11): 1179-1181.

Hanot, M., J. Hoarau, M. Carriere, J. F. Angulo and H. Khodja (2009). "Membrane-dependent bystander effect contributes to amplification of the response to alpha-particle irradiation in targeted and nontargeted cells." *Int J Radiat Oncol Biol Phys* **75**(4): 1247-1253.

ICRU (1983). *Microdosimetry*. Bethesda, Maryland, International Commission on Radiation Units and Measurements.

Kam, W. W. and R. B. Banati (2013). "Effects of ionizing radiation on mitochondria." *Free Radic Biol Med* **65**: 607-619.

Kim, G. J., K. Chandrasekaran and W. F. Morgan (2006). "Mitochondrial dysfunction, persistently elevated levels of reactive oxygen species and radiation-induced genomic instability: a review." *Mutagenesis* **21**(6): 361-367.

Kirkby, C. and E. Ghasroddashti (2015). "Targeting mitochondria in cancer cells using gold nanoparticle-enhanced radiotherapy: a Monte Carlo study." *Med Phys* **42**(2): 1119-1128.

Kukat, C., K. M. Davies, C. A. Wurm, H. Spahr, N. A. Bonekamp, I. Kuhl, F. Joos, P. L. Polosa, C. B. Park, V. Posse, M. Falkenberg, S. Jakobs, W. Kuhlbrandt and N. G. Larsson (2015). "Cross-strand binding of TFAM to a single mtDNA molecule forms the mitochondrial nucleoid." *Proc Natl Acad Sci U S A* **112**(36): 11288-11293.

Kukat, C. and N. G. Larsson (2013). "mtDNA makes a U-turn for the mitochondrial nucleoid." *Trends Cell Biol* **23**(9): 457-463.

Kukat, C., C. A. Wurm, H. Spahr, M. Falkenberg, N. G. Larsson and S. Jakobs (2011). "Super-resolution microscopy reveals that mammalian mitochondrial nucleoids have a uniform size and frequently contain a single copy of mtDNA." *Proc Natl Acad Sci U S A* **108**(33): 13534-13539.

Kundrať, P. and W. Friedland (2012). "Track structure calculations on intracellular targets responsible for signal release in bystander experiments with transfer of irradiated cell-conditioned medium." *Int J Radiat Biol* **88**(1-2): 98-102.

Leach, J. K., G. Van Tuyle, P. S. Lin, R. Schmidt-Ullrich and R. B. Mikkelsen (2001). "Ionizing radiation-induced, mitochondria-dependent generation of reactive oxygen/nitrogen." *Cancer Res* **61**(10): 3894-3901.

Liu, Z., W. V. Prestwich, R. D. Stewart, S. H. Byun, C. E. Mothersill, F. E. McNeill and C. B. Seymour (2007). "Effective target size for the induction of bystander effects in medium transfer experiments." *Radiat Res* **168**(5): 627-630.

May, A. and V. A. Bohr (2000). "Gene-specific repair of gamma-ray-induced DNA strand breaks in colon cancer cells: no coupling to transcription and no removal from the mitochondrial genome." *Biochem Biophys Res Commun* **269**(2): 433-437.

Mikkelsen, R. B. and P. Wardman (2003). "Biological chemistry of reactive oxygen and nitrogen and radiation-induced signal transduction mechanisms." *Oncogene* **22**(37): 5734-5754.

Nugent, S., C. E. Mothersill, C. Seymour, B. McClean, F. M. Lyng and J. E. Murphy (2010). "Altered mitochondrial function and genome frequency post exposure to  $\alpha$ -radiation and bystander factors." *Int J Radiat Biol* **86**(10): 829-841.

Nunnari, J. and A. Suomalainen (2012). "Mitochondria: in sickness and in health." *Cell* **148**(6): 1145-1159.

Prise, K. M. and J. M. O'Sullivan (2009). "Radiation-induced bystander signalling in cancer therapy." *Nat Rev Cancer* **9**(5): 351-360.

Rajendran, S., S. H. Harrison, R. A. Thomas and J. D. Tucker (2011). "The role of mitochondria in the radiation-induced bystander effect in human lymphoblastoid cells." *Radiat Res* **175**(2): 159-171.

Schmid, T. E., W. Friedland, C. Greubel, S. Girst, J. Reindl, C. Siebenwirth, K. Ilcic, E. Schmid, G. Multhoff, E. Schmitt, P. Kundrat and G. Dollinger (2015). "Sub-micrometer 20MeV protons or 45MeV lithium spot irradiation enhances yields of dicentric chromosomes due to clustering of DNA double-strand breaks." *Mutat Res Genet Toxicol Environ Mutagen* **793**: 30-40.

Schon, E. A., S. DiMauro and M. Hirano (2012). "Human mitochondrial DNA: roles of inherited and somatic mutations." *Nat Rev Genet* **13**(12): 878-890.

Selivanov, V. A., T. V. Votyakova, V. N. Pivtoraiko, J. Zeak, T. Sukhomlin, M. Trucco, J. Roca and M. Cascante (2011). "Reactive oxygen species production by forward and reverse electron fluxes in the mitochondrial respiratory chain." *PLoS Comput Biol* **7**(3): e1001115.

Szumiel, I. (2015). "Ionizing radiation-induced oxidative stress, epigenetic changes and genomic instability: the pivotal role of mitochondria." *Int J Radiat Biol* **91**(1): 1-12.

Wallace, D. C. (2005). "A mitochondrial paradigm of metabolic and degenerative diseases, aging, and cancer: a dawn for evolutionary medicine." *Annu Rev Genet* **39**: 359-407.

Yamamori, T., H. Yasui, M. Yamazumi, Y. Wada, Y. Nakamura, H. Nakamura and O. Inanami (2012). "Ionizing radiation induces mitochondrial reactive oxygen species production accompanied by upregulation of mitochondrial electron transport chain function and mitochondrial content under control of the cell cycle checkpoint." *Free Radic Biol Med* **53**(2): 260-270.

Zorov, D. B., M. Juhaszova and S. J. Sollott (2006). "Mitochondrial ROS-induced ROS release: an update and review." *Biochim Biophys Acta* **1757**(5-6): 509-517.

## Figure legends

Figure 1: The model of mitochondrial DNA (mtDNA) and mitochondria in PARTRAC in a perspective view by POVRAY™ raytracer software. Panel A: Basic 15nm box used as a building brick of the mtDNA model. The DNA double-helix is represented in atomic resolution. The TFAM proteins are not modelled explicitly in atomic resolution but as bending regions of the mtDNA only. The straight box shown here contains 326 bp of mtDNA and eight U-turns around TFAM proteins. Panel B: The model of a single mtDNA molecule is obtained by seamlessly stacking 52 basic boxes (20 straight and 32 bent ones). The whole 16.7 kbp closed loop is compacted into a nucleoid fitting into a cube with 80 nm side length. Panel C: 1000 mitochondria (yellow), with 10 mtDNA nucleoids each, are placed randomly in the cytoplasm of a model cell around the spherical nucleus (blue, with shadows from mitochondria). The nucleus contains a multi-scale model of nuclear DNA that ranges from DNA double-helix in atomic resolution over nucleosomes, 30 nm chromatin fiber, and chromatin domains to chromosomes, as described in detail previously (Friedland et al. 2011a).

Figure 2: Cumulative distribution of specific energies ('local doses') deposited to  $0.5 \mu\text{m}^3$  mitochondria (solid lines) or  $125 \mu\text{m}^3$  cell nuclei (dotted lines) by 2 mGy (red), 20 mGy (green), 0.2 Gy (cyan) or 2 Gy (black) of  $^{60}\text{Co}$   $\gamma$ -ray irradiation. To present the targets receiving low (or no at all) as well as those receiving high specific energies, the same results are plotted twice: Panel A: Fraction of mitochondria and cell nuclei with specific energies *below* the abscissa values. Since a single hit to a mitochondrion translates into specific energy of 4.8 mGy, the leftmost segments of the histograms depict the fraction of *non-hit* mitochondria. Panel B: Fraction of mitochondria and cell nuclei with specific energies *above* the abscissa values. The leftmost segments refer to the fraction of *hit* mitochondria.

Figure 3: Cumulative distribution of specific energies in mitochondria and cell nuclei due to 5 MeV  $\alpha$ -particle irradiation. Solid lines: results for mitochondria ( $0.5 \mu\text{m}^3$  volume), dotted lines: results for cell nuclei ( $125 \mu\text{m}^3$  volume); red: single particles that have hit the target volume, black: 1 Gy dose (fluence:  $0.061 \mu\text{m}^{-2}$ ). Panel A: Fraction of mitochondria or cell nuclei with specific energies *below* the abscissa values. Panel B: Fraction of mitochondria or cell nuclei with specific energies *above* the abscissa values.

Figure 4: Calculated small-scale DNA fragmentation patterns in mitochondrial DNA (mtDNA, solid lines) compared to nuclear DNA (nDNA, dotted lines) due to single tracks of 5 MeV  $\alpha$ -particles.

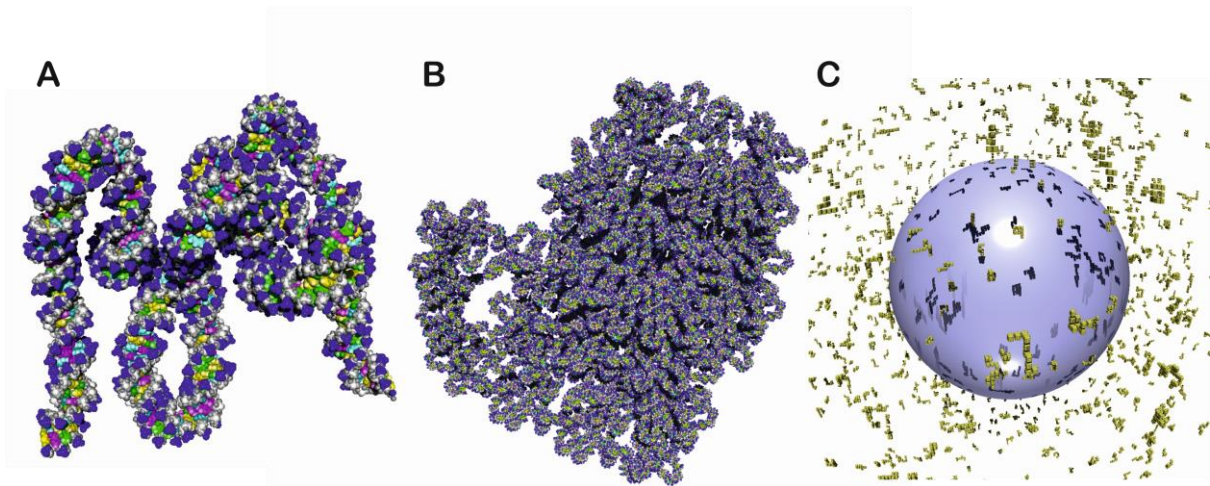


Figure 1

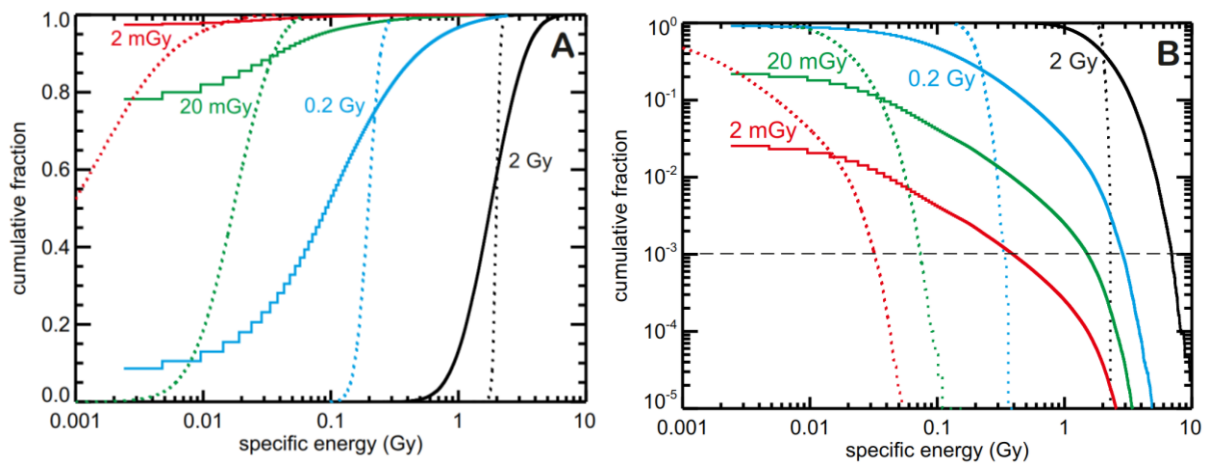


Figure 2

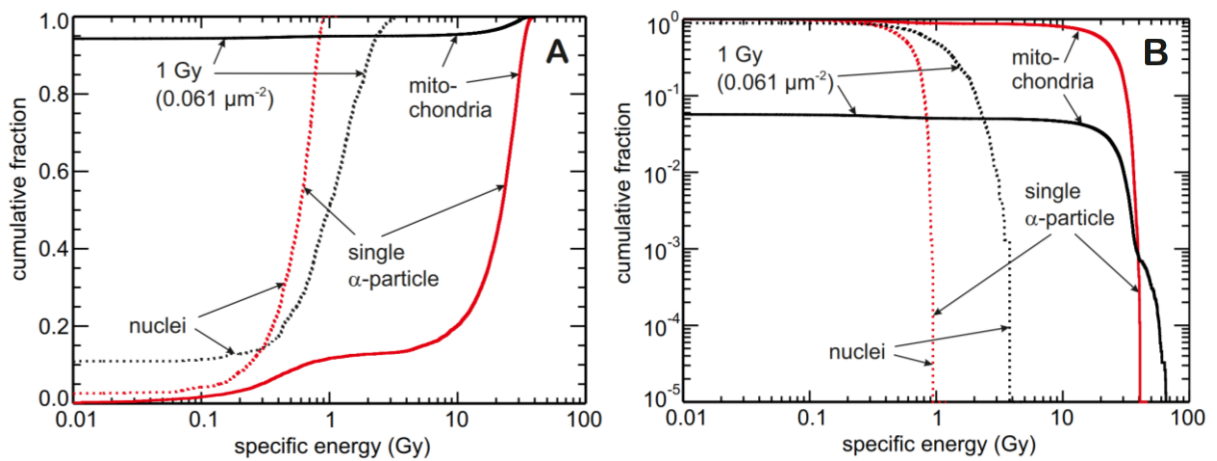


Figure 3

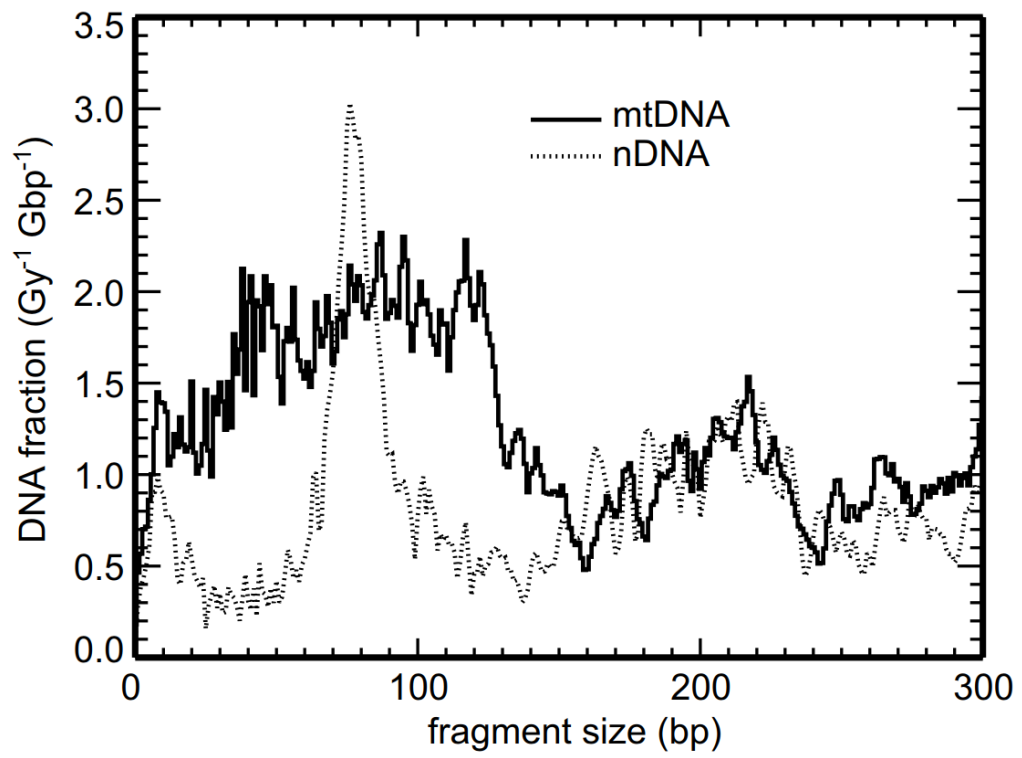


Figure 4

Table 1: Radiation-induced yields of damage to nuclear and mitochondrial DNA (nDNA and mtDNA, respectively) predicted by PARTRAC simulations. Scored have been single- and double-strand breaks to DNA (SSB and DSB, respectively). For nDNA, separately listed are damage yields from direct energy depositions and the total effect that includes DNA damage from radical attacks. For mtDNA, total effect is reported for three scenarios considered: (i) full scavenging of  $\cdot\text{OH}$  in mitochondria, corresponding to direct effects only, (ii) scavenging with  $\cdot\text{OH}$  lifetime of 2.5 ns as in the nucleus, and (iii) low scavenging without scavengers that would reduce  $\cdot\text{OH}$  lifetime, i.e. considering only water radiolysis and reactions with mtDNA.

Damage yields ( $\text{Gy}^{-1} \text{ Gbp}^{-1}$ )		nDNA		mtDNA, $\cdot\text{OH}$ scavenging:		
		Direct	Total	Full	Nuclear	Low
$^{60}\text{Co } \gamma$	SSB	52	170	50	185	258
	DSB	5.2	8.5	5.8	9.7	12.4
5 MeV $\alpha$	SSB	35	113	36	121	152
	DSB	13	19	15	23	26